Performance Bounds for Massive MIMO Uplink

Amin Khansefid and Hlaing Minn
Dept. of EE, University of Texas at Dallas, Richardson, TX, USA.

***Abstract*—In this paper, we consider massive MIMO uplink using maximum ratio combining (MRC) and zero forcing (ZF) receivers with perfect and imperfect channel state information (CSI). We derive lower and upper bounds on the achievable rates with arbitrary power allocation. Analytical and simulation results illustrate the accuracy and characteristics of the rate bounds.**

***Index Terms*—Massive MIMO, Imperfect CSI, Bound**

I. Introduction

The use of large number of antennas (a.k.a. massive MIMO) has recently emerged as a promising technology for enhancing spectrum efficiency and energy efficiency [1]–[4]. The very large signal space dimension of massive MIMO demands low complexity algorithms, e.g., linear detectors based on maximum ratio combining (MRC), zero forcing (ZF) or minimum mean-square error (MMSE) [2], [4]–[8]. As CSI plays a crucial role, the effect of imperfect CSI in massive MIMO is considered in [4]–[6].

A commonly used performance metric in the existing massive MIMO work is a lower bound of the achievable sum-rate conditioned on the large-scale fading coefficients of the users. [4] derives such lower bounds for ZF, MRC, and MMSE receivers under the scenario of equal power allocation among users. To develop a power allocation strategy or evaluate system performance with a certain power allocation strategy, a performance metric conditioned on the large-scale fading coefficients with arbitrary power allocation among the users is needed, and this paper develops such metrics. For the uplink of massive MIMO with ZF and MRC receivers under both scenarios of perfect and imperfect CSI, we derive lower and upper bounds of the achievable sum-rate conditioned on the large-scale fading coefficients of the users under arbitrary power allocation strategy.

Notation: Vectors (matrices) are denoted by bold face small (big) letters. The superscripts T, H, and $*$ stand for the transpose, complex conjugate transpose and conjugate of a matrix or vector, respectively. $\boldsymbol{I}_K$ is the $K \times K$ identity matrix. $\mathbb{E}\{\cdot\}$ and $\|.\|$ denote expectation and Euclidean norm, respectively. $\mathbf{n} \sim \mathcal{CN}(\mathbf{0}, \mathbf{C})$ means $\mathbf{n}$ is the zero-mean complex Gaussian vector with covariance matrix $\boldsymbol{C}$. $\mathcal{N}(0, \sigma^2)$ denotes zero-mean Gaussian random variable with variance σ^2. The exponential integral function is defined as $\mathrm{Ei}(x) \triangleq -\int_{-x}^{\infty} \frac{e^{-t}}{t} dt,\ x < 0$. δ_{ki} and $\Gamma(\cdot)$ denote the Kronecker delta and the Gamma function, respectively. $\mathrm{diag}\{a_1, \cdots, a_K\}$ means a diagonal matrix with diagonal elements $\{a_1, \cdots, a_K\}$.

II. System Model and Achievable Rates

We consider a single cell synchronized uplink multi-user MIMO system where K independent single-antenna users transmit data simultaneously on the same frequency band to a single BS with M antenna elements. We assume quasi-static frequency-flat channel gains, and channels of different users and antennas are independent. The overall $M \times K$ lowpass-equivalent channel matrix $\mathbf{G}$, whose (m,k)th element g_{mk} represents the gain of the channel from user k to base station antenna m, can be given as $\mathbf{G} = \mathbf{H}\mathbf{D}^{1/2}$ where $\mathbf{H}$ is an $M \times K$ matrix of i.i.d. $\mathcal{CN}(0,1)$ elements whose (m,k)th element h_{mk} represents the small-scale Rayleigh fading component of the channel between user k and BS antenna m, and $\mathbf{D}$ is a diagonal matrix with the kth diagonal element β_k relating to the large-scale fading component for user k. Thus, we have $g_{mk} = h_{mk}\sqrt{\beta_k}$. In the same way as in [4], we assume $\mathbf{D}$ is known at BS; this is well justified since $\{\beta_k\}$ change slowly and hence can be estimated reliably.

The data signal vector received from M antennas at BS, denoted by $M \times 1$ vector $\mathbf{y}$, is

$$\mathbf{y} = \mathbf{G}\mathbf{P}^{1/2}\mathbf{x} + \mathbf{n} \tag{1}$$

where $\mathbf{n} \sim \mathcal{CN}(\mathbf{0}, \mathbf{I}_M)$ is the noise vector, $\mathbf{P} \triangleq \mathrm{diag}\{p_1, \cdots, p_K\}$ with p_k denoting the transmit data power of user k, and $\mathbf{x} \triangleq [x_1, \cdots, x_K]^T$ with $\{x_k\}$ being i.i.d. data with $\mathbb{E}\left\{|x_k|^2\right\} = 1$. Thus, p_k equals data Tx SNR of user k.

We consider two linear receivers, MRC and ZF, which perform the following processing:

$$\mathbf{r} = \tilde{\mathbf{A}}^H \mathbf{y} \tag{2}$$

where $\tilde{\mathbf{A}}$ for the perfect CSI case is denoted by $\mathbf{A}$ and for the imperfect CSI case by $\hat{\mathbf{A}}$. $\mathbf{A}$ is given by $\mathbf{G}$ for MRC and $\mathbf{G}\left(\mathbf{G}^H\mathbf{G}\right)^{-1}$ for ZF. $\hat{\mathbf{A}}$ is obtained by substituting $\mathbf{G}$ with its estimate $\hat{\mathbf{G}}$ in $\mathbf{A}$. The kth element of $\mathbf{r}$, r_k, is the decision variable for detecting data of user k.

For channel estimation, each user transmits τ pilot symbols where $\tau \geq K$. Let $\mathbf{\Phi}$ denote the pilot matrix whose kth row is the pilot sequence of user k. We use orthogonal pilot sequences (i.e., $\mathbf{\Phi}\mathbf{\Phi}^H = \tau\mathbf{I}_K$) which yield easy and complete decoupling of different channels. The $M \times \tau$ received pilot matrix $\mathbf{Y}$ collected from M antennas over τ symbols is given by

$$\mathbf{Y} = \mathbf{G}\mathbf{Q}^{1/2}\mathbf{\Phi} + \mathbf{N} \tag{3}$$

where the noise matrix $\mathbf{N}$ has i.i.d. elements of $\mathcal{CN}(0,1)$ and $\mathbf{Q} \triangleq \mathrm{diag}\{q_1, \cdots, q_K\}$ with q_k denoting the transmit pilot power for user k. The MMSE estimate of $\mathbf{G}$ is

$$\hat{\mathbf{G}} = \mathbf{Y}\mathbf{\Phi}^H\mathbf{Q}^{-1/2}\tilde{\mathbf{D}} \tag{4}$$

where $\tilde{\mathbf{D}} \triangleq \left(\mathbf{D}^{-1}\mathbf{Q}^{-1} + \mathbf{I}_K\right)^{-1}$. The error matrix of channel estimation is defined as $\mathcal{E} \triangleq \hat{\mathbf{G}} - \mathbf{G}$. Due to the property of

978-1-4799-7088-9/14/$31.00 ©2014 IEEE

MMSE estimation in zero-mean Gaussian signal model, $\mathcal{E}$ and $\hat{\mathbf{G}}$ are independent, and the variance of each element of kth column of $\mathcal{E}$ is $\frac{\beta_k}{\tau q_k \beta_k + 1}$. All columns of $\hat{\mathbf{G}}$ are independent and the kth coulmn is $\hat{\mathbf{g}}_k \sim \mathcal{CN}\left(\mathbf{0}, \sigma^2_{\hat{\mathbf{g}}_k} \mathbf{I}_M\right)$ where

$$\sigma^2_{\hat{\mathbf{g}}_k} = \frac{\tau q_k \beta_k^2}{\tau q_k \beta_k + 1}. \tag{5}$$

With perfect CSI, we have r_k from (2) as

$$r_k = \sqrt{p_k}\mathbf{a}_k^H \mathbf{g}_k x_k + \sum_{i=1, i\neq k}^{K} \sqrt{p_i}\mathbf{a}_k^H \mathbf{g}_i x_i + \mathbf{a}_k^H \mathbf{n} \tag{6}$$

where $\mathbf{a}_k$ and $\mathbf{g}_k$ are kth columns of $\mathbf{A}$ and $\mathbf{G}$, respectively. If we assume the interference plus noise part of r_k is Gaussian, then the ergodic achievable rate of user k is

$$R_{\mathrm{P},k} = \mathbb{E}\left\{\log_2\left(1 + \gamma_{\mathrm{P},k}\right)\right\} \tag{7}$$

$$\text{where} \quad \gamma_{\mathrm{P},k} \triangleq \frac{p_k |\mathbf{a}_k^H \mathbf{g}_k|^2}{\sum_{i=1, i\neq k}^{K} p_i |\mathbf{a}_k^H \mathbf{g}_i|^2 + \|\mathbf{a}_k\|^2}, \tag{8}$$

otherwise, (7) is a lower bound. The subscript P refers to the perfect CSI case. As K increases, the Gaussian assumption becomes more accurate due to the central limit theorem.

For MRC receiver with perfect CSI, we have $\mathbf{a}_k = \mathbf{g}_k$, and (8) becomes

$$\gamma^{\mathrm{mrc}}_{\mathrm{P},k} = \frac{p_k \|\mathbf{g}_k\|^4}{\sum_{i=1, i\neq k}^{K} p_i |\mathbf{g}_k^H \mathbf{g}_i|^2 + \|\mathbf{g}_k\|^2}. \tag{9}$$

For ZF receiver with perfect CSI, we have $\mathbf{a}_k^H \mathbf{g}_i = \delta_{ki}$, and (8) simplifies to

$$\gamma^{\mathrm{zf}}_{\mathrm{P},k} = \frac{p_k}{\|\mathbf{a}_k\|^2}. \tag{10}$$

For the case of imperfect CSI, we have

$$\begin{aligned} r_k =& \sqrt{p_k}\hat{\mathbf{a}}_k^H \hat{\mathbf{g}}_k x_k + \sum_{i=1, i\neq k}^{K} \sqrt{p_i}\hat{\mathbf{a}}_k^H \hat{\mathbf{g}}_i x_i \\ &- \sum_{i=1}^{K} \sqrt{p_i}\hat{\mathbf{a}}_k^H \mathcal{E}_i x_i + \hat{\mathbf{a}}_k^H \mathbf{n} \end{aligned} \tag{11}$$

where $\hat{\mathbf{a}}_i$, $\hat{\mathbf{g}}_i$ and $\mathcal{E}_i$ are the ith columns of $\hat{\mathbf{A}}$, $\hat{\mathbf{G}}$, and $\mathcal{E}$, respectively. Including the overhead cost of pilots, the corresponding lower bound on ergodic capacity of user k is

$$R_{\mathrm{IP},k} = \mathbb{E}\left\{(1-\lambda)\log_2\left(1 + \gamma_{\mathrm{IP},k}\right)\right\} \tag{12}$$

where $\lambda \triangleq \frac{\tau}{T}$ with T being the total number of symbols in a transmission frame and

$$\gamma_{\mathrm{IP},k} \triangleq \frac{p_k |\hat{\mathbf{a}}_k^H \hat{\mathbf{g}}_k|^2}{\sum_{i=1, i\neq k}^{K} p_i |\hat{\mathbf{a}}_k^H \hat{\mathbf{g}}_i|^2 + \|\hat{\mathbf{a}}_k\|^2 \sum_{i=1}^{K} \frac{p_i \beta_i}{\tau q_i \beta_i + 1} + \|\hat{\mathbf{a}}_k\|^2} \tag{13}$$

The subscript IP refers to the imperfect CSI case.

For MRC receiver with imperfect CSI, we have $\hat{\mathbf{a}}_k = \hat{\mathbf{g}}_k$, and (13) reads as

$$\gamma^{\mathrm{mrc}}_{\mathrm{IP},k} = \frac{p_k \|\hat{\mathbf{g}}_k\|^4}{\sum_{i=1, i\neq k}^{K} p_i |\hat{\mathbf{g}}_k^H \hat{\mathbf{g}}_i|^2 + \|\hat{\mathbf{g}}_k\|^2 \sum_{i=1}^{K} \frac{p_i \beta_i}{\tau q_i \beta_i + 1} + \|\hat{\mathbf{g}}_k\|^2} \tag{14}$$

For ZF receiver with imperfect CSI, we still have $\hat{\mathbf{a}}_k^H \hat{\mathbf{g}}_i = \delta_{ki}$, and (13) becomes

$$\gamma^{\mathrm{zf}}_{\mathrm{IP},k} = \frac{p_k}{\left(1 + \sum_{i=1}^{K} \frac{p_i \beta_i}{\tau q_i \beta_i + 1}\right) \|\hat{\mathbf{a}}_k\|^2}. \tag{15}$$

III. Performance Bounds

Theorem 1. i) The lower bound on the rate of (7) for MRC receiver with perfect CSI is

$$\underline{R}^{\mathrm{mrc}}_{\mathrm{P},k} = \log_2\left(1 + \mathrm{SINR}^{\mathrm{mrc}}_{\mathrm{P},k}\right), \tag{16}$$

where we define the signal to interference-plus-noise ratio (SINR) for this case as follows:

$$\mathrm{SINR}^{\mathrm{mrc}}_{\mathrm{P},k} = \frac{p_k \beta_k (M-1)}{\sum_{i=1, i\neq k}^{K} p_i \beta_i + 1}. \tag{17}$$

ii) The lower bound on the rate of (12) for MRC receiver with imperfect CSI is

$$\underline{R}^{\mathrm{mrc}}_{\mathrm{IP},k} = (1-\lambda)\log_2\left(1 + \mathrm{SINR}^{\mathrm{mrc}}_{\mathrm{IP},k}\right), \tag{18}$$

where

$$\mathrm{SINR}^{\mathrm{mrc}}_{\mathrm{IP},k} = \frac{\tau p_k q_k \beta_k^2 (M-1)}{(\tau q_k \beta_k + 1)\left(1 + \sum_{i=1, i\neq k}^{K} p_i \beta_i\right) + p_k \beta_k}. \tag{19}$$

Theorem 2. i) The lower bound on the rate of (7) for ZF receiver with perfect CSI is

$$\underline{R}^{\mathrm{zf}}_{\mathrm{P},k} = \log_2\left(1 + \mathrm{SINR}^{\mathrm{zf}}_{\mathrm{P},k}\right) \tag{20}$$

$$\text{where} \quad \mathrm{SINR}^{\mathrm{zf}}_{\mathrm{P},k} = p_k \beta_k (M-K). \tag{21}$$

ii) The lower bound on the rate of (12) for ZF receiver with imperfect CSI is

$$\underline{R}^{\mathrm{zf}}_{\mathrm{IP},k} = (1-\lambda)\log_2\left(1 + \mathrm{SINR}^{\mathrm{zf}}_{\mathrm{IP},k}\right) \tag{22}$$

$$\text{where} \quad \mathrm{SINR}^{\mathrm{zf}}_{\mathrm{IP},k} = \frac{\tau p_k q_k \beta_k^2 (M-K)}{(\tau q_k \beta_k + 1)\left(1 + \sum_{i=1}^{K} \frac{p_i \beta_i}{\tau q_i \beta_i + 1}\right)}. \tag{23}$$

Proof: The same approach of [4] can be used to derive the above theorems. Thus, details are skipped. □

Remark 1. If data and pilot powers are scaled as $p_k = q_k = \frac{E}{\sqrt{M}}$, then lower bounds for MRC and ZF receivers in (18) and (22) approach a fixed rate as M increases to infinity:

$$\underline{R}_{\mathrm{IP},k} \to (1-\lambda)\log_2\left(1 + \tau E^2 \beta_k^2\right), \text{ as } M \to \infty. \tag{24}$$

Here our general bounds reduce to the same result in [4].

Next, we derive upper limit of achievable rates.

Theorem 3. i) The upper bound on the rate for MRC receiver and perfect CSI in (7) is

$$\bar{R}^{\mathrm{mrc}}_{\mathrm{P},k} = \log_2\left(1 - M\zeta_{\mathrm{P},k} \sum_{i=1, i\neq k}^{K} \theta_{i,k} e^{\frac{1}{\zeta_{\mathrm{P},i}}} \mathrm{Ei}\left(\frac{-1}{\zeta_{\mathrm{P,i}}}\right)\right) \tag{25}$$

where $\zeta_{\mathrm{P},i} \triangleq \beta_i p_i$ and $\theta_{i,k} \triangleq \frac{(\zeta_{\mathrm{P},i})^{K-3}}{\prod_{j=1, j\neq i, j\neq k}^{K} (\zeta_{\mathrm{P},i} - \zeta_{\mathrm{P},j})}$.

ii) For MRC receiver with imperfect CSI, the upper bound on (12) is given by

$$\bar{R}_{\mathrm{IP},k}^{\mathrm{mrc}} = (1-\lambda)\log_2\left(1 - M\zeta_{\mathrm{IP},k}\sum_{i=1,i\neq k}^{K}\hat{\theta}_{i,k}e^{\frac{\mu}{\zeta_{\mathrm{IP},i}}}\mathrm{Ei}(\frac{-\mu}{\zeta_{\mathrm{IP,i}}})\right) \tag{26}$$

where $\zeta_{\mathrm{IP},i} \triangleq \frac{\tau\beta_i^2 p_i q_i}{1+\tau\beta_i q_i}$, $\mu \triangleq 1+\sum_{i=1}^{K}\frac{\beta_i p_i}{1+\tau\beta_i q_i}$, and $\hat{\theta}_{i,k} \triangleq \frac{(\zeta_{\mathrm{IP},i})^{K-3}}{\prod_{j=1,j\neq i,j\neq k}^{K}(\zeta_{\mathrm{IP},i}-\zeta_{\mathrm{IP},j})}$.

For the proof, we use the following lemmas.

Lemma 1. Suppose $\{u_i\}_{i=1}^{K}$ are i.i.d. random variables with $u_i \sim \mathcal{CN}(0,1)$. For non-equal positive constants $\{\zeta_i\}_{i=1}^{K}$, if we define $z_k \triangleq \sum_{i=1,i\neq k}^{K}\zeta_i|u_i|^2$, then $\mathbb{E}\{\frac{1}{z_k+a}\} = -\sum_{i=1,i\neq k}^{K}\tilde{\theta}_{i,k}e^{\frac{a}{\zeta_i}}\mathrm{Ei}\left(-\frac{a}{\zeta_i}\right)$ where $\tilde{\theta}_{i,k} \triangleq \frac{(\zeta_i)^{K-3}}{\prod_{j=1,j\neq i,j\neq k}^{K}(\zeta_i-\zeta_j)}$.

Proof: Applying the approach in [9] yields the result. □

Lemma 2. For independent random vectors $\{\mathbf{x}_i\}_{i=1}^{K}$ with $\mathbf{x}_i \sim \mathcal{CN}(\mathbf{0},\sigma_i^2\mathbf{I}_M)$ and positive constants a, b and $\{c_i\}_{i=1}^{K}$, define $\gamma_k \triangleq \frac{b\|\mathbf{x}_k\|^4}{\sum_{i=1,i\neq k}^{K}c_i|\mathbf{x}_k^H\mathbf{x}_i|^2+a\|\mathbf{x}_k\|^2}$.Then when $c_i\sigma_i^2$ for $i=1,\cdots,K$ are unequal, we have $\mathbb{E}\{\gamma_k\} = -M\sigma_k^2 b\sum_{i=1,i\neq k}^{K}\tilde{\theta}_{i,k}e^{\frac{1}{\zeta_i}}\mathrm{Ei}(\frac{-1}{\zeta_i})$.

Proof: Define $\tilde{x}_i \triangleq \frac{\mathbf{x}_k^H\mathbf{x}_i}{\|\mathbf{x}_k\|}$, $i\neq k$. Then, $\tilde{x}_i \sim \mathcal{CN}(0,\sigma_i^2)$, and $\tilde{x}_i$ and $\mathbf{x}_k$ are independent [4]. So by defining $z_k \triangleq \sum_{i=1,i\neq k}^{K}c_i\sigma_i^2|u_i|^2$ where $\{u_i\}$ are i.i.d. with $\mathcal{CN}(0,1)$, we have $\mathbb{E}\{\gamma_k\} = \mathbb{E}\{b\|\mathbf{x}_k\|^2\}\mathbb{E}\left\{\frac{1}{z_k+a}\right\}$. First, $\|\mathbf{x}_k\|^2$ is central Chi-square with mean $M\sigma_k^2$. Next, applying Lemma 1 for $\mathbb{E}\left\{\frac{1}{z_k+a}\right\}$ yields the result. □

Proof of Theorem 3: i) By Jensen's inequality, the upper bound for (7) is given by $\bar{R}_{\mathrm{P},k}^{\mathrm{mrc}} \triangleq \log_2\left(1+\mathbb{E}\{\gamma_{\mathrm{P},k}^{\mathrm{mrc}}\}\right)$ where $\gamma_{\mathrm{P},k}^{\mathrm{mrc}}$ is given in (9). If we ignore the zero probability event that at least two $\zeta_{\mathrm{P},i}$'s are equal, by using Lemma 2 with $\mathbf{x}_i=\mathbf{g}_i$, $\sigma_i^2=\beta_i$, $b=p_k$, $a=1$, and $c_i=p_i$, we can compute $\mathbb{E}\left\{\gamma_{\mathrm{P},k}^{\mathrm{mrc}}\right\}$ and by substituting it into the equation of $\bar{R}_{\mathrm{P},k}^{\mathrm{mrc}}$ we complete the proof.

ii) Using Jensen's inequality, the upper bound for (12) is

$$\bar{R}_{\mathrm{IP},k}^{\mathrm{mrc}} \triangleq \log_2\left(1+\mathbb{E}\{\gamma_{\mathrm{IP},k}^{\mathrm{mrc}}\}\right). \tag{27}$$

From (14), we have $\gamma_{\mathrm{IP},k}^{\mathrm{mrc}} = \frac{p_k\|\hat{\mathbf{g}}_k\|^4}{\sum_{i=1,i\neq k}^{K}p_i|\hat{\mathbf{g}}_k^H\hat{\mathbf{g}}_i|^2+\mu\|\hat{\mathbf{g}}_k\|^2}$ where $\hat{\mathbf{g}}_k \sim (\mathbf{0},\sigma_{\hat{\mathbf{g}}_k}^2\mathbf{I}_M)$. If we ignore the zero probability event that at least two $\zeta_{\mathrm{IP},i}$'s are equal, by using Lemma 2 with $\mathbf{x}_i=\hat{\mathbf{g}}_i$, $\sigma_i^2=\sigma_{\hat{\mathbf{g}}_i}^2$, $b=p_k$, $a=\mu$, and $c_i=p_i$, we can compute $\mathbb{E}\left\{\gamma_{\mathrm{IP},k}^{\mathrm{mrc}}\right\}$ and by substituting it into (27) we complete the proof. □

Theorem 4. i) The upper bound on the rate of ZF receiver with perfect CSI is

$$\bar{R}_{\mathrm{P},k}^{\mathrm{zf}} = \log_2\left(1+\beta_k p_k(M-K+1)\right). \tag{28}$$

ii) The upper bound on the rate of ZF receiver with imperfect CSI is given by

$$\bar{R}_{\mathrm{IP},k}^{\mathrm{zf}} = \log_2\left(1+\frac{\tau p_k q_k\beta_k^2(M-K+1)}{(\tau q_k\beta_k+1)\left(1+\sum_{i=1}^{K}\frac{p_i\beta_i}{\tau q_i\beta_i+1}\right)}\right). \tag{29}$$

For the proof of theorem (4), we use the following lemma.

Lemma 3. For independent random vectors $\{\mathbf{x}_i\}_{i=1}^{K}$ with $\mathbf{x}_i \sim \mathcal{CN}(\mathbf{0},\sigma_i^2\mathbf{I}_M)$, define $\mathbf{X}$ as an $M\times K$ random matrix ($M\geq K$) with its ith column being $\mathbf{x}_i$ and $\mathbf{y}_i$ as ith column of $\mathbf{X}\left(\mathbf{X}^H\mathbf{X}\right)^{-1}$. Then $\mathbb{E}\left\{\frac{1}{\|\mathbf{y}_i\|^2}\right\} = \sigma_i^2(M-K+1)$.

Proof: We have $\|\mathbf{y}_i\|^2 = \left[\left(\mathbf{X}^H\mathbf{X}\right)^{-1}\right]_{ii}$. We can write $\mathbf{X}=\mathbf{H}\mathbf{\Lambda}$, where $\mathbf{H}$ is $M\times K$ matrix of i.i.d. $\mathcal{CN}(0,1)$ elements, and $\Lambda=\mathrm{diag}\{\sigma_1,\cdots,\sigma_K\}$. So $\left[\left(\mathbf{X}^H\mathbf{X}\right)^{-1}\right]_{ii} = \sigma_i^{-2}\left[\left(\mathbf{H}^H\mathbf{H}\right)^{-1}\right]_{ii}$. Let $v_i \triangleq \left(\left[\left(\mathbf{H}^H\mathbf{H}\right)^{-1}\right]_{ii}\right)^{-1}$. Then v_i has Gamma distribution with pdf $f_{v_i}(v) = \frac{v^{M-K}e^{-v}}{\Gamma(M-K+1)}$, $v>0$, [10], and $\mathbb{E}\{v_i\} = (M-K+1)$. Thus, $\mathbb{E}\left\{\frac{1}{\|\mathbf{y}_i\|^2}\right\} = \sigma_i^2\mathbb{E}\{v_i\} = \sigma_i^2(M-K+1)$. □

Proof of Theorem 4: i) By Jensen's inequality, the upper bound for (7) reads as $\bar{R}_{\mathrm{P},k}^{\mathrm{zf}} \triangleq \log_2\left(1+\mathbb{E}\{\gamma_{\mathrm{P},k}^{\mathrm{zf}}\}\right)$ where $\gamma_{\mathrm{P},k}^{\mathrm{zf}}$ is given in (10). Then using Lemma 3 with $\mathbf{x}_i=\mathbf{g}_i$, $\sigma_i^2=\beta_i$, and $\mathbf{y}_i=\mathbf{a}_i$, we obtain $\mathbb{E}\left\{\gamma_{\mathrm{P},k}^{\mathrm{zf}}\right\} = p_k\beta_k(M-K+1)$. Substituting it back into $\bar{R}_{\mathrm{P},k}^{\mathrm{zf}}$ completes the proof.

ii) With Jensen's inequality and $\gamma_{\mathrm{IP},k}^{\mathrm{zf}}$ given in (15), we obtain the upper bound for (12) as $\bar{R}_{\mathrm{IP},k}^{\mathrm{zf}} \triangleq \log_2\left(1+\mathbb{E}\{\gamma_{\mathrm{IP},k}^{\mathrm{zf}}\}\right)$ where $\mathbb{E}\left\{\gamma_{\mathrm{IP},k}^{\mathrm{zf}}\right\} = \frac{p_k}{1+\sum_{i=1}^{K}\frac{p_i\beta_i}{\tau q_i\beta_i+1}}\mathbb{E}\left\{\frac{1}{\|\hat{\mathbf{a}}_k\|^2}\right\}$. Using Lemma 3 with $\mathbf{x}_i=\hat{\mathbf{g}}_i$, $\sigma_i^2=\sigma_{\hat{\mathbf{g}}_i}^2$, and $\mathbf{y}_i=\hat{\mathbf{a}}_i$ yields $\mathbb{E}\left\{\frac{1}{\|\hat{\mathbf{a}}_k\|^2}\right\} = \frac{\tau\beta_k^2 q_k}{1+\tau\beta_k q_k}(M-K+1)$. Then substituting back into $\bar{R}_{\mathrm{IP},k}^{\mathrm{zf}}$ completes the proof. □

Remark 2. For ZF receiver, the difference between the lower and upper bounds, i.e., between (20), (22) and (28), (29), is the multiplicand inside the $\log_2$ function, namely $(M-K)$ versus $(M-K+1)$. Thus, for typical scenarios with $M>K$, both of the lower and upper bounds are very tight for all Tx SNR.

Remark 3. We can use average of analytical upper and lower bounds to approximate the actual rate. The results in Section IV will show this approximation is quite accurate.

IV. Simulation Results and Discussions

In the simulation, $K=10$ users are uniformly located in the disk around BS and the pdf of d_k, the distance of user k to BS, is given by $f_{d_k}(r) = \frac{2r}{d_m^2-d_0^2}$with $d_0=100\leq r\leq d_m=1000$. Small-scale channel fadings of users are i.i.d. Rayleigh distributed. For simulations with random large-scale fading, $\{\beta_k\}$ are independently generated by $\beta_k = z_k/(\frac{d_k}{d_0})^{\nu}$ where the path loss exponent is $\nu=3.8$ and z_k represents lognormal shadowing with $10\log_{10}(z_k) \sim \mathcal{N}\left(0,\sigma_{\mathrm{shadow,dB}}^2\right)$

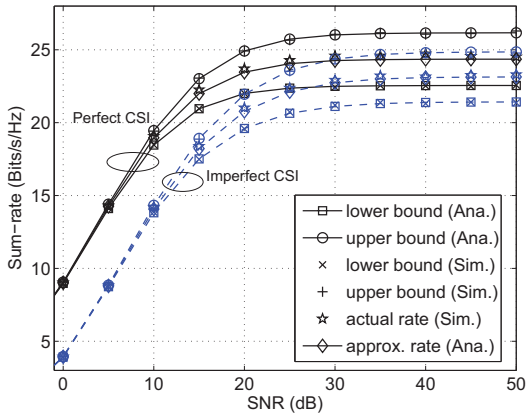

Fig. 1. Bounds of achievable rate versus Tx SNR for MRC receiver under fixed $\{\beta_k\}$. [$K = 10$ users, $M = 100$ antennas]

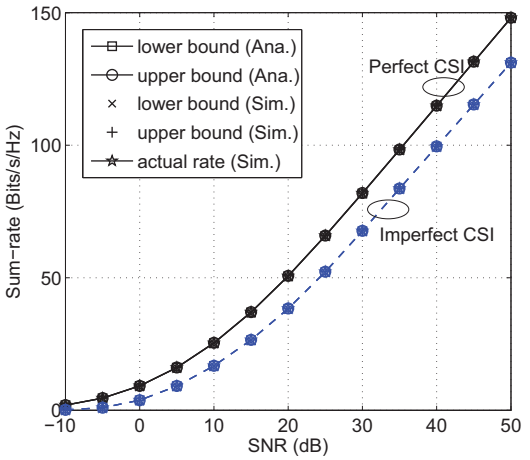

Fig. 2. Bounds of achievable rate versus Tx SNR for ZF receiver under fixed $\{\beta_k\}$. [$K = 10$ users, $M = 100$ antennas]

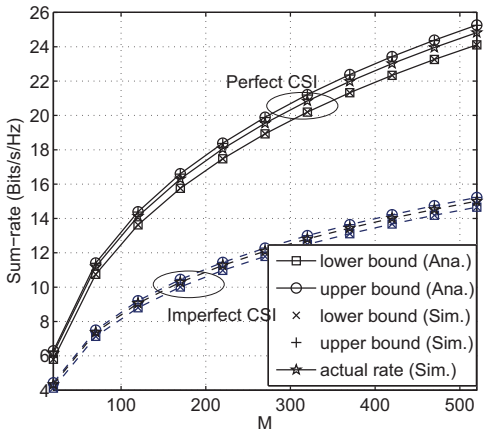

Fig. 3. Bounds of achievable rate versus the number of receive antennas, M, for MRC receiver. [$K = 10$ users, Tx SNR of 10 dB, random $\{\beta_k\}$]

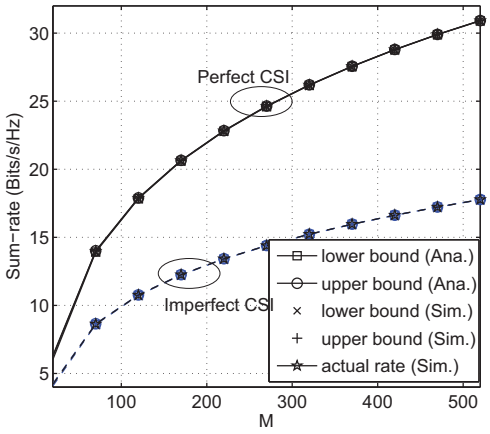

Fig. 4. Bounds of achievable rate versus the number of receive antennas, M, for ZF receiver. [$K = 10$ users, Tx SNR of 10 dB, random $\{\beta_k\}$]

and $\sigma_{\text{shadow,dB}}$ =8. The results are obtained by averaging over 1000 realizations of $\{\beta_k\}$. For simulations with fixed large-scale fading gains, we set $\beta_k = \beta_1 e^{-a(k-1)}$ with $\beta_1 = 0.1$ and $a = \ln(10)/3$. We use a frame length of $T = 200$ symbols.

A. Performance Bounds

We first verify the derived analytical bounds with their simulation results under the setting of fixed $\{\beta_k\}$, $M = 100$, and maximum power allocation. For comparison, we also include the actual rates (7) and (12) obtained by simulation as well as the approximate rates (average of the lower and upper bounds) in some figures. The sum-rate versus Tx SNR plots are shown in Fig. 1 for MRC receiver and in Fig. 2 for ZF receiver. The derived analytical bounds and their simulation results perfectly match. For MRC receiver, the bounds are quite tight for low to moderate Tx SNRs. At high Tx SNR, there are some gaps to the actual rates but the bounds still follow the same trend as the actual rate curve. For ZF receiver, the lower and upper bounds are very tight for all Tx SNRs (indistinguishable in the plots). The proposed approximate rate (as suggested in Remark 3) gives good approximation to the actual rate at all Tx SNRs for both MRC and ZF receivers.

Next, we present the results obtained by averaging over random $\{\beta_k\}$. The sum-rate versus Tx SNR plots show the same trends as in Fig. 1 and Fig. 2 and hence they are omitted. The plots of sum-rate versus M (the number of BS antennas) are shown in Fig. 3 and Fig. 4 at Tx SNR of 10 dB for MRC and ZF receiver, respectively. The approximate rate curve is omitted for presentation clarity. The previous discussion still holds. Furthermore, we observe that the accuracies of the bounds are not affected by M for both MRC and ZF receivers.

V. Conclusion

For massive MIMO uplink using MRC and ZF receivers with perfect and imperfect CSI, we have derived upper and lower bounds on achievable rates with arbitrary power allocation. The derived upper and lower bounds are very tight for ZF receiver at all SNRs and quite tight for MRC receiver at low and moderate SNRs. The average of the upper and lower bounds offers an accurate approximate of the actual rate for both receivers at all SNRs.

REFERENCES

[1] T. L. Marzetta, "Non-cooperative cellular wireless with unlimited numbers of base station antennas", *IEEE Trans. Wireless Commun.*, vol. 9, no. 11, pp. 3590–3600, Nov. 2010.

[2] F. Rusek, D. Persson, B. Kiong Lau, E. G. Larsson, T. L. Marzetta, O. Edfors, and F. Tufvesson, "Scaling up MIMO, opportunities and challenges with very large arrays", *IEEE Signal Process. Mag.*, vol. 30, no. 1, pp. 40–60, Jan. 2013.

[3] E. G. Larsson, F. Tufvesson, O. Edfors, and T. L. Marzetta, "Massive MIMO for next generation wireless systems," *IEEE Commun. Mag.*, vol. 52, no. 2, pp. 186-195, Feb. 2014.

[4] H. Q. Ngo, E. G. Larsson, T. L. Marzetta, "Energy and spectral efficiency of very large multiuser MIMO systems," *IEEE Trans. Commun.*, vol. 61, no. 4, pp. 1436–1449, Apr. 2013.

[5] H. Yang and T. L Marzetta, "Performance of conjugate and zero-forcing beamforming in large-scale antenna systems," *IEEE J. Selec. Area Commun.*, vol. 31, no. 2, pp. 172–179, Feb. 2013.

[6] J. Hoydis, S. ten Brink, and M. Debbah, "Massive MIMO in the UL/DL of cellular networks: how many antennas do we need?" *IEEE J. Selec. Areas Commun.*, vol. 31, no. 2, pp. 160–171, Feb. 2013.

[7] M. Matthaiou, C. Zhong, M. R. McKay, and T. Ratnarajah, "Sum rate analysis of ZF receivers in distributed MIMO systems", *IEEE J.Selec. Areas Commun.*, vol. 31, no. 2 , pp. 180–191, Feb. 2013.

[8] Y. C. Liang , G. Pan and Z. D. Bai "Asymptotic performance of MMSE receivers for large systems using random matrix theory", *IEEE Trans. Info. Theory*, vol. 53, no. 11, pp. 4173–4190, Nov. 2007.

[9] Y. Li, H. Minn, and J. Zeng, "An average Cramer-Rao bound for frequency offset estimation in frequency-selective fading channels," *IEEE Trans. Wireless Commun.*, vol. 9, no. 3, pp. 871–875, Mar. 2010.

[10] D. K. Nagar and A. K. Gupta, "Expectations of functions of complex Wishart matrix," *Acta Appl. Math.*, vol. 113, no. 3, pp. 265–288, Mar. 2011.